



Universiteit  
Leiden  
The Netherlands

## **Extravascular inflammation in experimental atherosclerosis : the role of the liver and lungs**

Wong, M.C.

### **Citation**

Wong, M. C. (2013, May 14). *Extravascular inflammation in experimental atherosclerosis : the role of the liver and lungs*. Retrieved from <https://hdl.handle.net/1887/20879>

Version: Corrected Publisher's Version

License: [Licence agreement concerning inclusion of doctoral thesis in the Institutional Repository of the University of Leiden](#)

Downloaded from: <https://hdl.handle.net/1887/20879>

**Note:** To cite this publication please use the final published version (if applicable).

Cover Page



Universiteit Leiden



The handle <http://hdl.handle.net/1887/20879> holds various files of this Leiden University dissertation.

**Author:** Wong, Man Chi

**Title:** Extravascular inflammation in experimental atherosclerosis : the role of the liver and lungs

**Issue Date:** 2013-05-14

## Hepatocyte-Specific IKK $\beta$ Activation Enhances VLDL-Triglyceride Production in *APOE\*3*-Leiden Mice

Janna A. van Diepen<sup>1</sup>, Man C. Wong<sup>2</sup>, Bruno Guigas<sup>3</sup>, Jasper Bos<sup>1</sup>, Rinke Stienstra<sup>5</sup>, Leanne Hodson<sup>6</sup>, Steven E. Shoelson<sup>7</sup>, Jimmy F.P. Berbée<sup>1</sup>, Patrick C.N. Rensen<sup>1</sup>, Johannes A. Romijn<sup>1,a</sup>, Louis M. Havekes<sup>1,4,8</sup>, Peter J. Voshol<sup>1,b</sup>

Depts. of <sup>1</sup>Endocrinology and Metabolic Diseases, <sup>2</sup>Pulmonology, <sup>3</sup>Molecular Cell Biology and <sup>4</sup>Cardiology, Leiden University Medical Center, Leiden, The Netherlands; <sup>5</sup>Dept. of General Internal Medicine, Radboud University Medical Center, Nijmegen, The Netherlands; <sup>6</sup>Oxford Centre for Diabetes, Endocrinology and Metabolism, University of Oxford, Churchill Hospital, Oxford, UK; <sup>7</sup>Joslin Diabetes Center and the Department of Medicine, Harvard Medical School, Boston, Massachusetts, USA; <sup>8</sup>Netherlands Organization for Applied Scientific Research – Biosciences, Gaubius Laboratory, Leiden, The Netherlands; <sup>a</sup>Present address: Dept. of Internal Medicine, University of Amsterdam, Amsterdam, The Netherlands; <sup>b</sup>Present address: Metabolic Research Laboratories, Institute of Metabolic Science, University of Cambridge, Cambridge, UK.

*J Lipid Res* 2011;52(5):942-950

---

## Abstract

Low-grade inflammation in different tissues, including activation of the nuclear factor- $\kappa$ B (NF- $\kappa$ B) pathway in liver, is involved in metabolic disorders such as type 2 diabetes and cardiovascular diseases (CVD). In this study we investigated the relation between chronic hepatocyte-specific overexpression of IKK $\beta$  and hypertriglyceridemia, an important risk factor for CVD, by evaluating whether activation of IKK $\beta$  only in the hepatocyte affects VLDL-triglyceride (TG) metabolism directly. Transgenic overexpression of constitutively active human I $\kappa$ B kinase (IKK $\beta$ ) specifically in hepatocytes of hyperlipidemic *APOE\*3-Leiden* mice clearly induced hypertriglyceridemia. Mechanistic *in vivo* studies revealed that the hypertriglyceridemia was caused by increased hepatic VLDL-TG production, rather than a change in plasma VLDL-TG clearance. Studies in primary hepatocytes showed that IKK $\beta$  overexpression also enhances TG secretion *in vitro*, indicating a direct relation between IKK $\beta$  activation and TG production within the hepatocyte. Hepatic lipid analysis and hepatic gene expression analysis of pathways involved in lipid metabolism suggested that hepatocyte-specific IKK $\beta$  overexpression increases VLDL production not by increased steatosis or decreased FA oxidation, but most likely by ChREBP-mediated upregulation of *Fas* expression. These findings implicate that specific activation of inflammatory pathways exclusively within hepatocytes induces hypertriglyceridemia. Furthermore, we identify the hepatocytic IKK $\beta$  pathway as a possible target to treat hypertriglyceridemia.

---

## Introduction

Obesity is associated with diseases such as dyslipidemia, type 2 diabetes and cardiovascular disease (CVD). The accumulation of lipids in numerous tissues is accompanied by increased inflammatory processes, such as macrophage infiltration and production of inflammatory mediators in white adipose tissue. In liver, fat accumulation increases the activity of the pro-inflammatory nuclear factor- $\kappa$ B (NF- $\kappa$ B), and liver-specific activation of NF- $\kappa$ B induces metabolic disturbances.<sup>1,2</sup>

Hypertriglyceridemia is caused by accumulation of VLDL particles in the plasma as a consequence of changes in lipid metabolism that are associated with obesity. Pro-inflammatory cytokines can cause hypertriglyceridemia<sup>3</sup> and, conversely, suppression of inflammation may reduce hypertriglyceridemia<sup>4</sup> suggesting a direct causal role for inflammatory pathways in the development of hypertriglyceridemia. In fact, administration of lipopolysaccharide (LPS), an inflammatory component of the outer membrane of Gram-negative bacteria, increases plasma triglyceride (TG) levels.<sup>5</sup> However, many inflammatory mediators affect multiple tissues, such as muscle, adipose tissue and liver and, moreover, they can act on multiple cell types including macrophages. The specific contribution of hepatocytes in the relation between inflammation and TG metabolism has never been studied.

In the current study we, therefore, aimed to investigate whether activation of the inflammatory NF- $\kappa$ B pathway exclusively in hepatocytes affects VLDL-TG metabolism and, as a consequence, causes hypertriglyceridemia. To this end, we used hepatocyte-specific transgenic IKK $\beta$  (*LIKK*) mice, which have been described before.<sup>1</sup> *LIKK* mice have an albumin promoter to drive expression of constitutively active human I $\kappa$ B kinase  $\beta$  (IKK $\beta$ ), which activates the NF- $\kappa$ B pathway selectively in hepatocytes. To study the effects of the hepatocyte-specific inflammation on VLDL-TG metabolism, we crossbred the *LIKK* mouse with the transgenic *APOE\*3-Leiden* (*E3L*) mouse that expresses human *APOE\*3-Leiden* (a mutant form of APOE3) and human *APOC1*,<sup>6</sup> both of which attenuate the clearance of apoE-containing TG-rich lipoproteins. Therefore, the *E3L* mouse shows increased plasma TG and cholesterol levels and is a well-established model of human-like lipoprotein metabolism.<sup>7</sup> By using the *E3L.LIKK* mouse, we were able to study the effects of the inflammatory NF- $\kappa$ B pathway in the hepatocyte on TG-rich lipoprotein metabolism directly. Our results show that activation of NF- $\kappa$ B in hepatocytes of *E3L* mice induces hypertriglyceridemia by enhancing VLDL-TG production directly within hepatocytes.

---

## Materials and methods

### Animals

*LIKK* mice, which express constitutively active human IKK $\beta$  selectively in hepatocytes under control of the albumin promoter<sup>1</sup> were crossbred with *E3L* mice,<sup>6</sup> expressing both human *APOE\*3-Leiden* and human *APOC1*, in our animal facility to obtain heterozygous *E3L.LIKK* mice on a C57Bl/6J background. Male *E3L.LIKK* and *E3L* littermates were housed under standard conditions with a 12-hour light-dark cycle and were fed a standard mouse chow diet with free

access to water. Experiments were performed in 14-week old animals after an overnight fast. All experiments were approved by the institutional ethical committee on animal care and experimentation.

### **Western blot analysis**

Tissues were homogenized by Ultraturrax (22,000 rpm; 2x5 sec) in an ice-cold buffer (pH 7.4) containing 30 mM Tris.HCl, 150 mM NaCl, 10 mM NaF, 1 mM EDTA, 1 mM  $\text{Na}_3\text{VO}_4$ , 0.5% (v/v) Triton X-100, 1% (v/v) SDS and protease inhibitors (Complete, Roche, Mijdrecht, The Netherlands) at a 1:6 (w/v) ratio. Homogenates were centrifuged (16,000 rpm; 15 min, 4°C) and the protein content of the supernatant was determined using the BCA protein assay kit (Pierce, Rockford, IL). Proteins (20-50  $\mu\text{g}$ ) were separated by 7-10% SDS-PAGE followed by transfer to a polyvinylidene fluoride (PVDF) membrane. Membranes were blocked for 1 h at room temperature in Tris-buffered saline with Tween-20 (TBST) with 5% non-fat dry milk followed by an overnight incubation with the following antibodies: p-Ser536 NF- $\kappa\text{B}$  p65 (#3031), NF- $\kappa\text{B}$  p65 (#3034), p-Ser32/36 I $\kappa\text{B}\alpha$  (#9246), I $\kappa\text{B}\alpha$  (#9242) (all from Cell Signaling), MTP (#612022) (BD Biosciences, Erembodegem, Belgium) and DGAT1 (#54037) (Abcam, Cambridge, UK). Blots were then incubated with a horseradish peroxidase (HRP)-conjugated secondary antibodies for 1 h at room temperature. Bands were visualized by enhanced chemiluminescence (ECL) and quantified using Image J (NIH).

### **Plasma lipids and lipoprotein profiles**

Blood was collected from the tail vein into chilled paraoxon (Sigma, St Louis, MO)-coated capillaries to prevent ongoing lipolysis.<sup>8</sup> Capillaries were placed on ice, centrifuged and plasma was assayed for TG, total cholesterol (TC), and phospholipids (PL) using commercially available enzymatic kits from Roche Molecular Biochemicals (Indianapolis, IN). Free fatty acids (FFA) were measured using NEFA-C kit from Wako Diagnostics (Instruchemie, Delfzijl, The Netherlands). For the determination of lipid distribution over plasma lipoproteins, 50  $\mu\text{L}$  of pooled plasma was used for fast performance liquid chromatography (FPLC). Plasma was injected onto a Superose 6 column (Äkta System; Amersham Pharmacia Biotech, Piscataway, NJ), and eluted at a constant flow rate of 50  $\mu\text{L}/\text{min}$  with PBS pH 7.4. TG and TC were measured as described above in collected fractions of 50  $\mu\text{L}$ .

### **Liver lipids**

Lipids were extracted from livers according to a modified protocol from Bligh and Dyer.<sup>9</sup> Briefly, a small piece of liver was homogenized in ice-cold methanol. After centrifugation, lipids were extracted by addition of 1800  $\mu\text{L}$   $\text{CH}_3\text{OH}:\text{CHCl}_3$  (3:1 v/v) to 45  $\mu\text{L}$  homogenate. The  $\text{CHCl}_3$  phase was dried and dissolved in 2% Triton X-100. Hepatic TG and TC concentrations were measured using commercial kits as described earlier. Liver lipids were expressed per mg protein, which was determined using the BCA protein assay kit.

### **FA composition of liver TG**

Liver samples (100 mg) were homogenized with 0.5 mL saline. Subsequently, 5 mL of chloroform: methanol (2:1 by volume) was added containing butylated hydroxytoluene (BHT).

In addition, an internal TG standard was added before extraction. Liver lipids were extracted according to the method of Folch *et al.*<sup>10</sup> Total TG were separated by spotting lipid extracts onto silica gel 60 (Merck) thin-layer chromatography plates and running in hexane: diethyl ether: acetic acid (85: 15: 1, v/v/v). Lipid bands were visualized under UV light after spraying with 0.1% ANS (8-anilino-1-naphthalene sulfonic acid), and identified using commercial standards. TG bands were scraped into glass tubes and methylated at 80°C with 1.5% H<sub>2</sub>SO<sub>4</sub> in methanol for 2 h. TG-derived FA were eluted into hexane. Separation and quantification of the FA methyl esters (FAMES) from liver TG was achieved using gas chromatography, on an Agilent 6890 GC (Agilent Technologies, UK) fitted with a 30 m x 0.53 mm (film thickness 1 µm) capillary column (RTX-Wax). Individual FA peaks were identified by a reference containing known FAMES. FA compositions (mol%) were then determined.

### Generation of VLDL-like emulsion particles

VLDL-like TG-rich emulsion particles were prepared and characterized as described previously.<sup>11,12</sup> Lipids (100 mg) at a weight ratio of triolein: egg yolk phosphatidylcholine: lysophosphatidylcholine: cholesteryl oleate: cholesterol of 70: 22.7: 2.3: 3.0: 2.0, supplemented with 200 µCi of glycerol tri[9,10(n)-<sup>3</sup>H]oleate ([<sup>3</sup>H]TO) were sonicated at 10 µm output using a Soniprep 150 (MSE Scientific Instruments, Crawley, UK). Density gradient ultracentrifugation was used to obtain 80 nm-sized emulsion particles, which were used for subsequent experiments. TG content of the emulsions was measured as described above. Emulsions were stored at 4°C under argon and used within 7 days.

### *In vivo* clearance of VLDL-like emulsion particles

To study the *in vivo* clearance of the VLDL-like emulsion particles, overnight fasted mice were anesthetized by intraperitoneal injection of acepromazine (6.25 mg/kg Neurotranq, Alfasan International BV, Weesp, The Netherlands), midazolam (6.25 mg/kg Dormicum, Roche Diagnostics, Mijdrecht, The Netherlands), and fentanyl (0.31 mg/kg Janssen Pharmaceuticals, Tilburg, The Netherlands). Mice were injected (t=0) via the tail vein with 200 µL of [<sup>3</sup>H]TO-labeled emulsion particles at a dose of 100 µg of TG per mouse. Blood samples were taken from the tail vein at 1, 2, 5, 10 and 15 minutes after injection and plasma <sup>3</sup>H-activity was counted. Plasma volumes were calculated as 0.04706 x body weight (g) as determined from <sup>125</sup>I-BSA clearance studies as described previously.<sup>13</sup> After taking the last blood sample, the liver, heart, spleen, muscle and white adipose tissue (*i.e.* gonadal, subcutaneous and visceral) were collected. Organs were dissolved overnight at 60°C in Tissue Solubilizer (Amersham Biosciences, Roosendaal, The Netherlands) and <sup>3</sup>H-activity was counted. Uptake of [<sup>3</sup>H]TO-derived radioactivity by the organs was calculated from the <sup>3</sup>H activity in each organ divided by plasma-specific activity of [<sup>3</sup>H]TG and expressed per mg wet tissue weight.

### *In vivo* hepatic VLDL-TG and VLDL-apoB production

To measure VLDL production *in vivo*, mice were fasted overnight and anesthetized as described above. Mice were injected intravenously with Tran<sup>35</sup>S label (150 µCi/mouse; MP Biomedicals, Eindhoven, The Netherlands) to label newly produced apolipoprotein B (apoB). After 30 minutes,

at t=0 min, Triton WR-1339 (Sigma-Aldrich) was injected intravenously (0.5 mg/g body weight, 10% solution in PBS) to block serum VLDL clearance. Blood samples were drawn before (t=0) and 15, 30, 60 and 90 min after injection and used for determination of plasma TG concentration as described above. After 120 min, mice were exsanguinated via the retro-orbital plexus and euthanized by cervical dislocation. VLDL was isolated from serum after density gradient ultracentrifugation at  $d < 1.006$  g/mL by aspiration<sup>14</sup> and counted for incorporated <sup>35</sup>S-activity.

### **Isolation of primary mouse hepatocytes**

Primary hepatocytes were isolated from mouse livers according to the method of Berry and Friend<sup>15</sup> modified by Groen *et al.*<sup>16</sup> Briefly, the portal vein was cannulated and liver was first perfused with a calcium-free Krebs/bicarbonate buffer, saturated with 95% O<sub>2</sub> and 5% CO<sub>2</sub> at a flow rate of 5 mL/min. Subsequently, perfusion of the liver was continued with calcium-containing Krebs/bicarbonate buffer with 0.0125% collagenase (Roche, Penzberg, Germany) during 10-15 min until cellular dissociation was observed. Cells were gently released and centrifuged four times at 50g for 1 min at 4°C to remove non-parenchymal cells from pelleted hepatocytes. Isolated hepatocytes were washed and suspended in complete Williams' E medium containing insulin (Actrapid), fetal calf serum, dexamethasone and penicillin/streptomycin (P/S). Hepatocytes were isolated with similar yields from livers of *E3L.LIKK* and *E3L* mice, 70-80% viable, as assessed by trypan blue dye exclusion, and 99% free of non-parenchymal cells by visual inspection. No differences with respect to viability were observed between cells isolated from *E3L.LIKK* and *E3L* mice. Cells were seeded into 12-well dishes, pre-coated with collagen at a density of  $1.0 \times 10^6$  viable cells/well in 2 mL complete Williams' E medium. After a 2 h adherence period, non-attached cells were removed from the cultures by careful washing.

### ***In vitro* measurement of TG secretion by hepatocytes**

TG secretion *in vitro* was measured as described previously.<sup>17</sup> After an overnight incubation, cells were washed 2 times and incubated 4 h in fetal calf serum-free and hormone-free (SF-HF) Williams' E medium. To measure rates of secretion of TG, cells were subsequently incubated in SF-HF medium containing 4.4  $\mu$ Ci of [<sup>3</sup>H]glycerol (Amersham; UK) with or without 0.75 mM oleate (C18:1) complexed with BSA to stimulate lipogenesis. After 1, 2, 4 or 20 h incubation, medium was collected and cells were washed three times and harvested in 2 mL PBS. Lipids were extracted from medium according to a modified protocol from Bligh and Dyer.<sup>9,17</sup> The lipids were dried under nitrogen, dissolved into chloroform with 2 mM tripalmitin added as a carrier and subjected to TLC (Silica gel 60, Merck, Belgium) using hexane: diethylether: acetic acid (80/20/1; v/v/v) as mobile phase. Lipid spots were visualized using iodine vapor, and tripalmitin-positive spots were scraped off, dissolved in 0.5 M acetic acid, and assayed for radioactivity by scintillation counting. Protein content of the cells was determined using the BCA protein assay kit as described earlier. Data are expressed as dpm/mg protein.

### **Hepatic gene expression analysis**

Total RNA was extracted from liver tissues using the Nucleospin RNA II kit (Macherey-Nagel, Düren, Germany) according to manufacturer's instructions. RNA quality of each sample was examined by lab-on-a-chip technology using Experion Std Sens analysis kit (Biorad, Hercules,

CA, USA). One  $\mu\text{g}$  of total RNA was reverse-transcribed with iScript cDNA synthesis kit (Bio-Rad) and the obtained cDNA was purified with Nucleospin Extract II kit (Macherey-Nagel). Real-Time PCR was carried out on the IQ5 PCR machine (Biorad) using the Sensimix SYBR Green RT-PCR mix (Quantace, London, UK). mRNA levels were normalized to mRNA levels of cyclophilin (*Cyclo*) and glyceraldehyde-3-phosphate dehydrogenase (*Gapdh*). Primer sequences are listed in Supplemental Table S1.

### Statistical analysis

Data are presented as means  $\pm$  SD. Statistical differences were calculated using the Mann-Whitney *U* test for two independent samples with SPSS 16.0 (SPSS Inc, Chicago, IL).  $P < 0.05$  was regarded statistically significant.

## Results

### *LIKK* increases liver NF- $\kappa$ B signaling in *E3L* mice

To verify that *LIKK* expression in *E3L* mice increases hepatic NF- $\kappa$ B signaling, livers from *E3L* and *E3L.LIKK* mice were assayed for the presence of phosphorylated over total NF- $\kappa$ B and  $\text{I}\kappa\text{B}\alpha$  using Western blot (Fig. 1). Indeed, expression of *LIKK* increased the ratio of pNF- $\kappa$ B Ser<sup>536</sup> over NF- $\kappa$ B ( $1.6 \pm 0.4$  fold;  $P < 0.05$ ) (Fig. 1A, B) as well as that of p $\text{I}\kappa\text{B}\alpha$  Ser<sup>32/36</sup> over  $\text{I}\kappa\text{B}\alpha$  ( $1.9 \pm 0.6$  fold;  $P < 0.05$ )

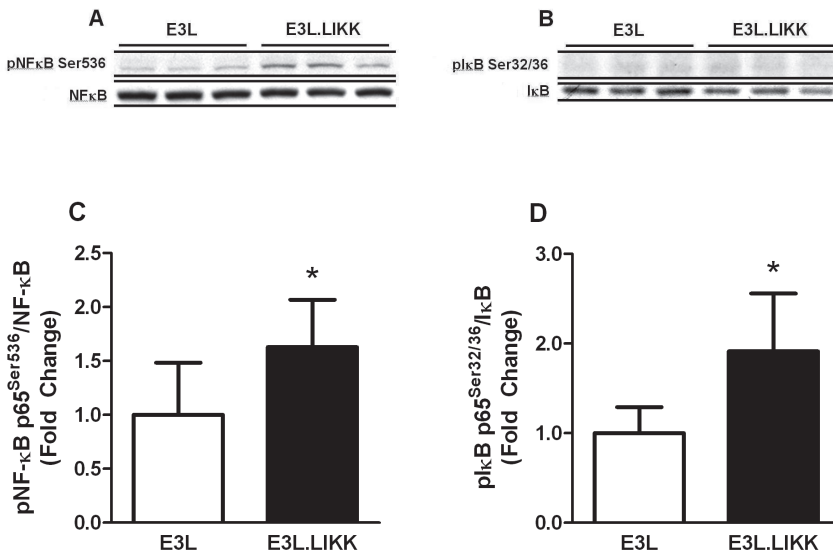


**Fig. 1.** *LIKK* increases hepatic NF- $\kappa$ B signaling in *E3L* mice. *E3L* and *E3L.LIKK* mice were fed a chow diet and sacrificed at the age of 14 weeks after an overnight fast. NF- $\kappa$ B signaling was measured in liver tissue by phosphorylation of NF- $\kappa$ B (A,C) and  $\text{I}\kappa\text{B}$  (B,D). Representative Western blots of phosphorylated NF- $\kappa$ B (NF- $\kappa$ B Ser<sup>536</sup>) and total NF- $\kappa$ B (A) and phosphorylated  $\text{I}\kappa\text{B}\alpha$  (p $\text{I}\kappa\text{B}\alpha$  Ser<sup>32/36</sup>) and total  $\text{I}\kappa\text{B}\alpha$  (B) are shown for 3 mice per group. Ratios of phosphorylated proteins over total proteins were quantified (B,D). Values are means  $\pm$  SD (n=5-7). \* $P < 0.05$ .

(Fig. 1C, D). The increased ratio of  $pI\kappa B\alpha$  Ser<sup>32/36</sup> over  $I\kappa B\alpha$  was mainly caused by a decrease of total  $I\kappa B\alpha$  ( $0.8\pm 0.1$  fold;  $P<0.05$ ), indicating increased  $I\kappa B\alpha$  ubiquitination and degradation by the proteasome, which reflects activation of the NF- $\kappa B$  pathway. These data are in line with the increased NF- $\kappa B$  signaling previously observed in *LIKK* mice as compared to wild-type (WT) mice.<sup>1</sup>

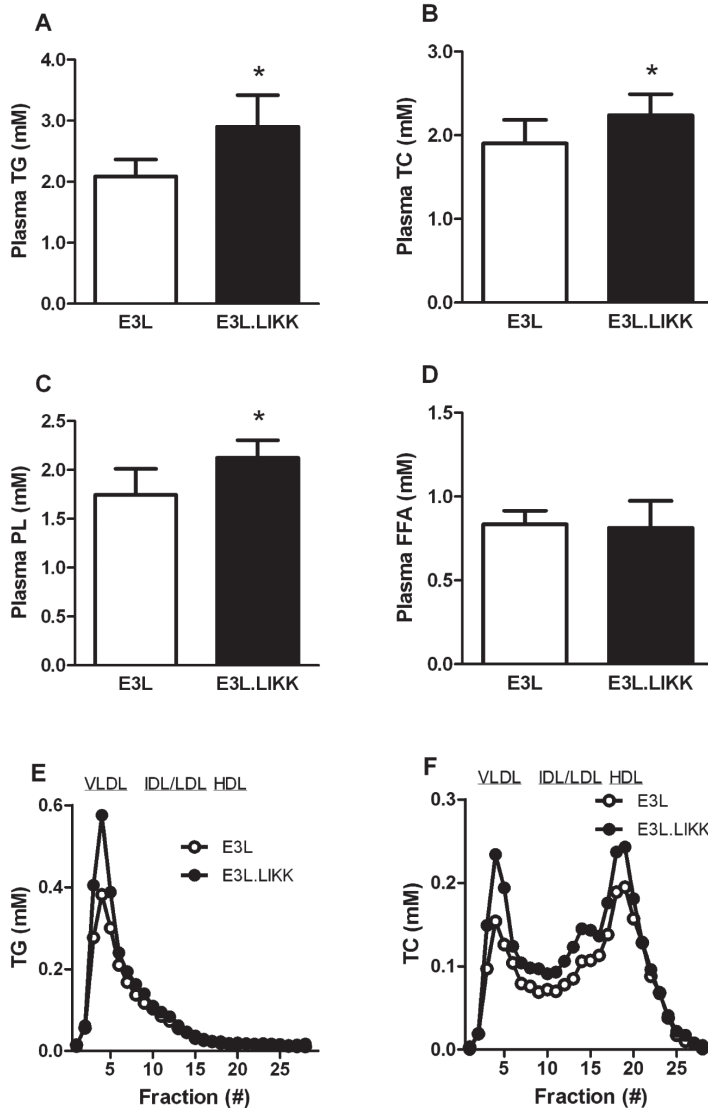


**Fig. 2.** *LIKK* induces hyperlipidemia in *E3L* mice. Plasma triglycerides (TG) (A), total cholesterol (TC) (B), phospholipids (PL) (C) and free fatty acid (FFA) (D) levels were measured in plasma of overnight fasted *E3L* and *E3L.LIKK* mice. Values are means  $\pm$  SD ( $n=5-7$ ). \* $P<0.05$ . Plasma was collected, pooled per group, and subjected to FPLC to separate lipoproteins. Distribution of TG (E) and TC (F) over lipoproteins was determined.

### **LIKK induces hypertriglyceridemia in E3L mice**

To determine whether the hepatocyte-specific inflammation affects plasma lipid levels, TG, TC, PL and FFA levels were measured in plasma of *E3L* and *E3L.LIKK* mice (Fig. 2). *LIKK* expression in *E3L* mice increased TG by +39% ( $2.90 \pm 0.52$  vs  $2.09 \pm 0.28$  mmol/L;  $P < 0.05$ ; Fig. 2A), TC by +18% ( $2.24 \pm 0.25$  vs  $1.90 \pm 0.28$  mmol/L;  $P < 0.05$ ; Fig. 2B), and PL by +22% ( $2.12 \pm 0.18$  vs  $1.74 \pm 0.27$  mmol/L;  $P < 0.05$ ; Fig. 2C). *LIKK* did not affect plasma FFA levels (Fig. 2D). Lipoprotein profiling showed that the *LIKK*-induced increase in plasma TG could be explained by a rise in VLDL-TG (+42%) (Fig. 2E). Likewise, the increase in TC was mainly reflected by an increase in VLDL-C (+54%), LDL-C (+34%) and HDL-C (+25%) (Fig. 2F).

### **LIKK does not affect clearance of VLDL-like emulsion particle-TG in E3L mice**

Hypertriglyceridemia is caused by a decrease in VLDL-TG clearance and/or an increase in hepatic VLDL-TG production. To investigate whether *LIKK* inhibits the clearance of VLDL-TG, the plasma clearance and organ distribution of [<sup>3</sup>H]TO-labeled TG-rich VLDL-like emulsion particles was evaluated in *E3L.LIKK* versus *E3L* mice (Fig. 3). *LIKK* did not affect the plasma half-life of [<sup>3</sup>H]TO (Fig. 3A), nor the uptake of [<sup>3</sup>H]TO-derived fatty acids (FA) by the various organs (Fig. 3B), indicating that *LIKK* does not increase plasma TG levels by decreasing TG clearance.

### **LIKK increases VLDL-TG production in E3L mice**

As no difference was observed in TG clearance between *E3L.LIKK* and *E3L* mice, it is likely that the *LIKK*-induced increase in plasma TG levels can be explained by an increase of VLDL-TG production. The rate of hepatic VLDL-TG production was measured by determining plasma TG levels after intravenous Triton WR1339 injection (Fig. 4). Indeed, *LIKK* strongly increased the accumulation of plasma TG at all time points (Fig. 4A). The VLDL-TG production rate,

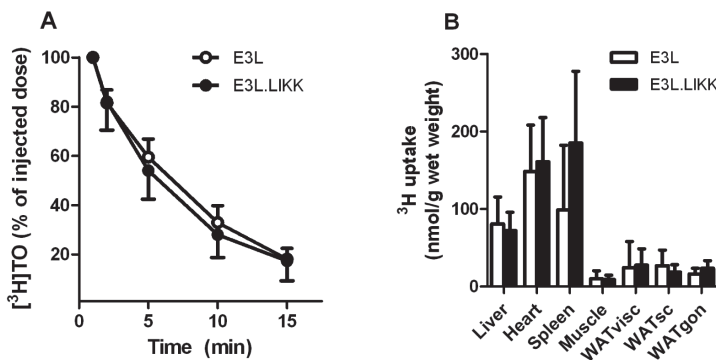


**Fig. 3.** *LIKK* does not affect clearance of VLDL-like emulsion particle-TG in *E3L* mice. *E3L* and *E3L.LIKK* mice that were fasted overnight were injected with [<sup>3</sup>H]TO-labeled VLDL-like emulsion particles. Blood was collected at the indicated time points and radioactivity was measured in plasma (A) of *E3L* mice (open circles) and *E3L.LIKK* mice (closed circles). Uptake of [<sup>3</sup>H]TO-derived activity by various organs was determined, and total FA uptake was calculated from the specific activity of TG in plasma, and expressed as nmol FA per mg wet tissue weight (B). Values are means  $\pm$  SD (n=8). WAT, white adipose tissue; visc, visceral; sc, subcutaneous; gon, gonadal.

as determined from the slope of the curve from all individual mice, was increased by +48% ( $3.90 \pm 1.01$  vs  $2.64 \pm 0.82$  mM/h,  $P < 0.05$ ) (Fig. 4B), whereas the rate of VLDL-apoB production did not change significantly ( $P = 0.52$ ) (Fig. 4C). Since each VLDL particle contains a single apoB molecule, *LIKK* apparently increases plasma TG levels by enhancing VLDL-TG production without affecting VLDL particle production.

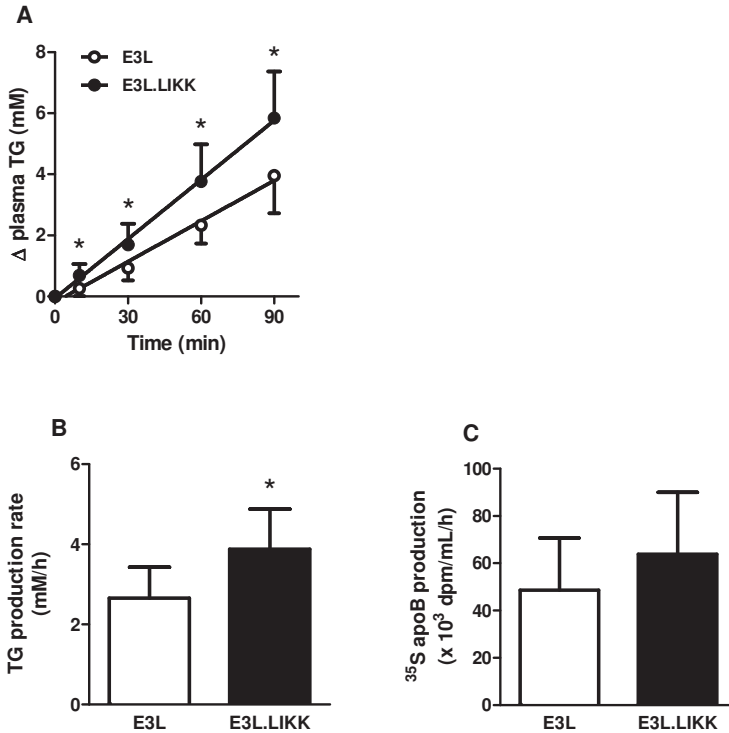


**Fig. 4.** *LIKK* increases VLDL-TG production in *E3L* mice. *E3L* and *E3L.LIKK* mice were fasted overnight and injected with Trans $^{35}\text{S}$  ( $t = -30$  min) and Triton WR1339 ( $t = 0$ ) and blood samples were drawn at the indicated time points. TG concentrations were determined in plasma of *E3L* mice (open circles) and *E3L.LIKK* mice (closed circles), and plotted as the increase in plasma TG relative to  $t = 0$  (A). The rate of TG production was calculated from the slopes of the curves from the individual mice (B). After 120 min, VLDL was isolated by ultracentrifugation,  $^{35}\text{S}$ -activity was counted, and the production rate of newly synthesized VLDL- $^{35}\text{S}$ -apoB was determined (C). Values are means  $\pm$  SD ( $n = 5-8$ ). \* $P < 0.05$ .

### *LIKK* does not affect liver lipid levels

To investigate whether the increase in hepatic VLDL-TG production was the result of increased lipid substrate availability in the liver, the effect of *LIKK* on the hepatic lipid content was investigated (Fig. 5). However, *E3L* and *E3L.LIKK* mice did not differ with respect to liver TG levels (Fig. 5A) and TC levels (Fig. 5B). *LIKK* did not influence the FA composition of hepatic TG, apart from a mild increase in the relative abundance of linoleic acid (18:2 n-6) by +19% ( $P < 0.05$ ) (Suppl. Fig. S1).

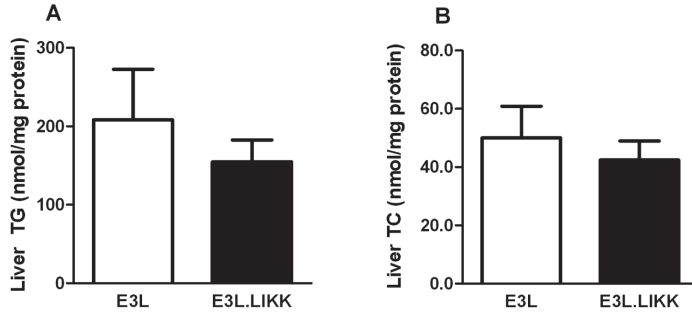


**Fig. 5.** *LIKK* does not affect liver lipid content in *E3L* mice. Livers were obtained from overnight fasted *E3L* and *E3L.LIKK* mice and lipids were extracted. Triglycerides (TG, A) and total cholesterol (TC, B) concentrations were measured and expressed per mg protein. Values are means  $\pm$  SD (n=5-7). \* $P$ <0.05.

### ***LIKK* directly increases TG secretion in hepatocytes from *E3L* mice**

To evaluate whether  $IKK\beta$  overexpression in hepatocytes directly increases VLDL-TG production, we next studied TG secretion from isolated hepatocytes of *E3L* and *E3L.LIKK* mice *in vitro*. We used [ $^3$ H]glycerol as precursor for TG synthesis, by measuring the accumulation of [ $^3$ H]TG in the medium (Fig. 6). In the absence of oleate, the [ $^3$ H]TG secretion was low, but *LIKK* significantly increased the [ $^3$ H]TG secretion after 20 h of incubation as compared to the [ $^3$ H]TG secretion from control *E3L* hepatocytes (2.3-fold;  $P$ <0.05) (Fig. 6A). In the presence of oleate, as a substrate for TG synthesis, [ $^3$ H]TG secretion was markedly increased, and *LIKK* caused an additional increase in [ $^3$ H]TG secretion, reaching significance after 20 h of incubation (1.9-fold at 20 h;  $P$ <0.05) (Fig. 6B).

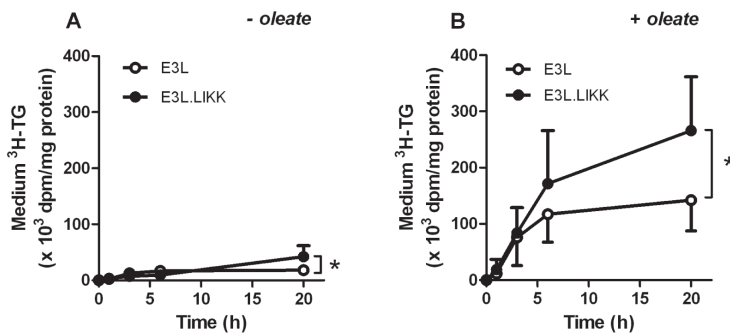


**Fig. 6.** *LIKK* increases TG secretion in hepatocytes from *E3L* mice. Hepatocytes were isolated from *E3L* (open circles) and *E3L.LIKK* mice (closed circles), cultured overnight, and incubated without or with oleate complexed with bovine serum albumin. [ $^3$ H]Glycerol was added to quantify newly synthesized triacylglycerols. Medium was collected at the indicated time points, [ $^3$ H]TG was measured and expressed as dpm per mg cell protein. Values are means  $\pm$  SD of 3-6 mice per group, *in vitro* experiments were performed in triplicate (n=3-6). \* $P$ <0.05.

### **LIKK increases hepatic expression of fatty acid synthase, but does not affect protein levels or expression of genes involved in VLDL production**

To obtain further insight into the mechanism underlying the effects of IKK $\beta$  overexpression on VLDL-TG production, we evaluated the hepatic expression of genes involved in VLDL secretion, lipogenesis, FA oxidation, cholesterol metabolism, bile acid metabolism, lipid droplets and

**Table 1.** Effect of *LIKK* on hepatic expression of genes involved in lipid metabolism in *E3L* mice.

Gene	Protein	<i>E3L</i>	<i>E3L.LIKK</i>	Change
<b>VLDL secretion</b>				
<i>ApoB</i>	ApoB	1.00 $\pm$ 0.35	1.01 $\pm$ 0.34	n.s.
<i>Mttp</i>	MTP	1.00 $\pm$ 0.46	1.34 $\pm$ 0.36	n.s.
<b>Lipogenesis</b>				
<i>Srebp-1c</i>	SREBP1c	1.00 $\pm$ 0.39	1.10 $\pm$ 0.74	n.s.
<i>Dgat1</i>	DGAT1	1.00 $\pm$ 0.32	1.21 $\pm$ 0.41	n.s.
<i>Fas</i>	FAS	1.00 $\pm$ 0.52	2.43 $\pm$ 1.07**	+143%
<b>FA oxidation</b>				
<i>Acox1</i>	ACO	1.00 $\pm$ 0.70	1.13 $\pm$ 0.20	n.s.
<i>Cpt1a</i>	CPT1a	1.00 $\pm$ 0.58	0.95 $\pm$ 0.23	n.s.
<b>Glucose metabolism</b>				
<i>Pklr</i>	L-PK	1.00 $\pm$ 0.48	1.72 $\pm$ 0.80*	+72%
<b>Cholesterol metabolism</b>				
<i>Abcg5</i>	ABCG5	1.00 $\pm$ 0.22	1.05 $\pm$ 0.31	n.s.
<i>Abcg8</i>	ABCG6	1.00 $\pm$ 0.16	0.93 $\pm$ 0.16	n.s.
<i>Hmgcr</i>	HMG-CoA	1.00 $\pm$ 0.19	0.98 $\pm$ 0.08	n.s.
<b>Bile acid metabolism</b>				
<i>Cyp7a1</i>	CYP7A1	1.00 $\pm$ 0.59	1.19 $\pm$ 0.55	n.s.
<i>Cyp8b1</i>	CYP8B1	1.00 $\pm$ 0.60	1.21 $\pm$ 0.27	n.s.
<i>Cyp27a1</i>	CYP27A1	1.00 $\pm$ 0.41	1.85 $\pm$ 0.51**	+85%
<b>Lipid droplets</b>				
<i>Plin2</i>	PLIN2/ADRP	1.00 $\pm$ 0.98	1.04 $\pm$ 0.33	n.s.
<i>Plin5</i>	PLIN5/PAT-1	1.00 $\pm$ 0.72	1.64 $\pm$ 0.55*	+64%
<i>Cidec</i>	CIDE-3/FSP27	1.00 $\pm$ 0.98	1.05 $\pm$ 0.42	n.s.
<i>Cidea</i>	CIDEA	1.00 $\pm$ 0.65	0.85 $\pm$ 0.59	n.s.
<b>Transcription factors</b>				
<i>Ppara</i>	PPAR $\alpha$	1.00 $\pm$ 0.28	0.89 $\pm$ 0.16	n.s.
<i>Ppargc1b</i>	PGC-1 $\beta$	1.00 $\pm$ 0.63	0.77 $\pm$ 0.26	n.s.
<i>Nr1h3</i>	LXR $\alpha$	1.00 $\pm$ 0.35	1.09 $\pm$ 0.09	n.s.
<i>Nr1h4</i>	FXR	1.00 $\pm$ 0.50	1.58 $\pm$ 0.43*	+58%

Livers were isolated from overnight fasted *E3L* and *E3L.LIKK* mice. mRNA was isolated and mRNA expression of the indicated genes was quantified by RT-PCR. Data are calculated as fold difference as compared to the control group. Values are means  $\pm$  SD (n=8). \* $P$ <0.05 and \*\* $P$ <0.01 compared to the control group. n.s., not significant. *Abcg5*, ATP-binding cassette sub-family G member 5; *Abcg8*, ATP-binding cassette sub-family G member 8; *Acox1*, acyl-coenzyme A oxidase 1; *ApoB*, apolipoprotein B; *Cidea*, cell death activator CIDE-A; *Cidec*, fat-specific protein FSP27; *Cpt1a*, carnitine palmitoyltransferase 1a; *Cyp27a1*, cholesterol 27 hydroxylase; *Cyp7a1*, cholesterol 7 alpha hydroxylase; *Cyp8b1*, sterol 12 alpha-hydroxylase; *Dgat1*, diglyceride acyltransferase 1; *Fas*, fatty acid synthase; *Hmgcr*, HMG-CoA reductase; *Mttp*, microsomal triglyceride transfer protein; *Nr1h3*, liver X receptor alpha; *Nr1h4*, farnesoid X activated receptor; *Pklr*, liver-type pyruvate kinase; *Plin2*, perilipin 2; *Plin5*, perilipin 5; *Ppara*, peroxisome proliferator activated receptor alpha; *Ppargc1b*, PPAR-gamma coactivator 1-beta; *Srebp-1c*, sterol-regulatory element binding protein.

nuclear receptors in livers of *E3L* and *E3L.LIKK* mice (Table 1). Even though *LIKK* induced an increase of VLDL-TG production *in vivo* and *in vitro*, *LIKK* did not affect hepatic gene expression or protein level (Suppl. Fig. S2A,B) of microsomal TG transfer protein (*Mttp*), which is involved in the assembly and secretion of VLDL. In addition, *LIKK* did not affect apoB (*ApoB*) expression, in line with the observation that *LIKK* did not increase VLDL-apoB secretion *in vivo*. Also, *LIKK* did not affect expression of sterol regulatory element binding protein 1c (*Srebp-1c*), which regulates genes required for *de novo* lipogenesis, nor did it affect expression or protein levels (Suppl. Fig. S2A,C) of acyl:diacylglycerol transferase 1 (*Dgat1*), which catalyzes the final and only committed step in TG synthesis.

In addition, *LIKK* did not largely affect clusters of genes involved in FA oxidation (acyl-coenzyme A oxidase 1 (*Acox1*) and carnitine palmitoyltransferase 1a (*Cpt1a*), cholesterol metabolism (ATP-binding cassette sub-family G member 5 (*Abcg5*), ATP-binding cassette sub-family G member 8 (*Abcg8*) and HMG-CoA reductase (*Hmgcr*) or bile acid metabolism (cholesterol 7 alpha hydroxylase (*Cyp7a1*) and sterol 12 alpha-hydroxylase (*Cyp8b1*)), apart from a 1.9-fold increase in cholesterol 27 hydroxylase (*Cyp27a1*) expression. Additionally, *LIKK* did not affect clusters of genes involved in lipid droplet formation (perilipin 2 (*Plin2*), fat-specific protein FSP27 (*Cidec*) and cell death activator CIDE-A (*Cidea*)), or expression of nuclear receptors (peroxisome proliferator activated receptor alpha (*Ppara*), PPAR-gamma coactivator 1-beta (*Ppargc1*) and liver X receptor alpha (*Nr1h3*)), apart from a 1.6-fold increase in expression of perilipin 5 (*Plin5*) and farnesoid X activated receptor (*Nr1h4*) respectively.

However, *LIKK* did increase expression of FA synthase (*Fas*), which plays a key role in FA synthesis, by 2.4-fold, and of liver-type pyruvate kinase (*Pklr*) by 1.7-fold, both of which are target genes of ChREBP. Taken together, these data suggest that *LIKK* increases VLDL-TG production by ChREBP-mediated upregulation of *Fas* expression, suggesting an increase in *de novo* lipogenesis.

---

## Discussion

Obesity leads to an increase in inflammatory processes in numerous organs including the liver.<sup>18</sup> In the current study, we questioned whether increased activation of inflammatory pathways in the liver, specifically in hepatocytes, induces hypertriglyceridemia. Indeed, we show that chronic activation of the inflammatory NF- $\kappa$ B pathway specifically in hepatocytes increases plasma TG, which was caused by an increased VLDL-TG production rather than a decreased clearance of VLDL-TG. Furthermore, we provide evidence that the increased TG production induced by hepatocyte-specific IKK $\beta$  overexpression is a direct effect of the transgene expression in the hepatocyte.

The strong relation between inflammation and hypertriglyceridemia has largely been derived from the observed increase in plasma TG during acute infection, which is believed to contribute to the host defense.<sup>19</sup> However, although similar inflammatory pathways are involved, metabolic inflammation is clearly different from acute inflammation with respect to its cause, intensity and duration. The inflammation that is observed in obesity, is a chronic and low-grade inflammation that is caused by a metabolic overload, rather than a pathogen.<sup>20</sup> The NF- $\kappa$ B

activity in the liver of *E3L.LIKK* mice in this study is about 1.5-fold higher compared to control *E3L* mice, which is similar to hepatic NF- $\kappa$ B activation levels seen after HFD feeding and in obesity.<sup>1</sup> The present study shows that this low-grade activation of hepatocyte-specific IKK $\beta$  induces an increase in plasma TG levels in *E3L* mice, a model for human-like lipoprotein metabolism, which was due to an increase in plasma VLDL-TG levels. Additional investigation of VLDL-TG metabolism revealed that the increased VLDL-TG levels were not caused by decreased clearance of TG from VLDL-like particles, but rather by increased hepatic production of VLDL-TG. These findings are in line with a study showing that injection of a low dose of LPS increases secretion of VLDL-TG, without affecting its clearance.<sup>5</sup> However, LPS associates with macrophages rather than with hepatocytes,<sup>21</sup> which hampers interpretation which cell type is primarily responsible for the increase in VLDL-TG secretion. In addition to LPS, individual cytokines, that activate various cell types, increase VLDL-TG production.<sup>3,22</sup> Since both LPS and cytokines can activate NF- $\kappa$ B signaling, our findings could suggest that the increase in VLDL secretion caused by LPS and cytokines in these earlier studies has been mediated, at least in part, via direct or indirect activation of NF- $\kappa$ B in the hepatocytes. In the present study, even though *LIKK* clearly increased VLDL-TG secretion, there were no significant effects of *LIKK* on apoB production or hepatic *ApoB* gene expression. This suggests that NF- $\kappa$ B activation increases the intracellular lipidation of apoB, but not the number of VLDL-particles secreted. This is in contrast with a study of Tsai *et al.*,<sup>23</sup> showing that adenoviral-mediated overexpression of IKK did increase apoB secretion in HepG2 cells. This discrepancy could possibly be explained by the level of IKK overexpression, which was higher with adenoviral-mediated IKK overexpression in their *in vitro* HepG2 model than with transgenic overexpression in our *in vivo* study. It is thus reasonable to postulate that low-grade NF- $\kappa$ B activity mainly increases lipidation of the VLDL particles, whereas a higher degree of NF- $\kappa$ B activation could in addition increase the number of secreted VLDL-particles.

It is interesting to speculate about the mechanism why hepatocyte-specific NF- $\kappa$ B activation increases VLDL-TG secretion, as many different factors could theoretically be involved. For example, IKK $\beta$  overexpression can cause insulin resistance,<sup>1</sup> which could result in an inability of insulin to suppress VLDL-TG production.<sup>24</sup> Furthermore, Kupffer cells have been suggested to play an important role in hepatic lipid metabolism.<sup>25</sup> Additionally, Kupffer cell products could possibly suppress lipid oxidation in hepatocytes via NF- $\kappa$ B mediated suppression of PPAR $\alpha$  activity.<sup>26</sup> Furthermore, although plasma FFA levels were unaltered by *LIKK*, liver-directed FA flux may have been influenced, resulting in altered substrate availability for VLDL-TG production. Therefore, to evaluate the effect of IKK $\beta$  overexpression in hepatocytes on VLDL-TG production in absence of these potentially confounding factors, we studied the effect of IKK $\beta$  in hepatocytes on TG production *in vitro*. In fact, IKK $\beta$  expression in hepatocytes *per se* appeared to directly increase VLDL-TG production. Although additional factors may contribute to the effect of *LIKK* on VLDL-TG production *in vivo*, a direct effect of IKK $\beta$  overexpression in hepatocytes thus at least contributes to this phenomenon.

PPAR $\alpha$ , LXR and FXR have shown to be activated during inflammation and interact with inflammatory processes<sup>27,28</sup> and could possibly underlie the mechanism by which hepatocyte-specific NF- $\kappa$ B activation increases VLDL-TG secretion directly within the hepatocyte. However, no change was observed in expression of hepatic PPAR $\alpha$  and LXR or expression of their target

genes. NF- $\kappa$ B activation did increase FXR expression, but FXR activation has been linked to a lower VLDL-TG secretion,<sup>29</sup> making a causal relationship between FXR activation and the increase in VLDL-TG secretion unlikely. Apparently, chronic hepatocyte-specific activation of NF- $\kappa$ B by IKK $\beta$  overexpression does not induce identical changes in lipogenic pathways that are seen in acute inflammation, however, it clearly increases VLDL-TG production and induces hypertriglyceridemia. Increased hepatic lipid availability, by increased lipogenesis and/or decreased lipid oxidation, could also underlie the mechanism by which hepatocyte-specific NF- $\kappa$ B increases VLDL-TG secretion. Acute inflammation has been shown to increase hepatic lipogenesis as measured by incorporation of  $^3\text{H}_2\text{O}$  into FA *in vivo*.<sup>5,30,31</sup> In our study we measured expression of genes involved in hepatic FA oxidation and *de novo* lipogenesis. Despite the fact that *LIKK* did not decrease the expression of genes involved in FA oxidation, *LIKK* clearly increased expression of *Fas*, which is a key enzyme in the regulation of FA synthesis. Although upregulation of *Fas* could be mediated by the transcription factors LXR, Srebp-1c and ChREBP,<sup>32,33</sup> the observed upregulation of *Pklr* as a main ChREBP target gene suggests that *LIKK* most likely activates ChREBP, thereby increasing *Fas* expression. The fact that activation of NF- $\kappa$ B has been linked to local disturbances in glucose metabolism that could activate ChREBP would underscore this observation.<sup>1,34,35</sup> It is thus conceivable that increased ChREBP mediated *Fas* expression increases hepatic lipogenesis and thereby increases lipid availability for VLDL-TG production.<sup>36</sup> In fact, activation of lipogenesis results in large, but not more, VLDL particles, which is consistent with our findings.<sup>37</sup> The fact that we did not observe an increase in the hepatic TG content or FA oxidation that could have been expected by increased *Fas* expression,<sup>38</sup> can be explained by efficient incorporation of newly synthesized TG into nascent VLDL resulting in the increased hepatic VLDL-TG secretion.

In conclusion, we show that activation of hepatocyte-specific NF- $\kappa$ B through overexpression of IKK $\beta$  increases TG levels in *E3L* mice by stimulation of VLDL-TG secretion, directly within the hepatocyte, without effects on VLDL-TG clearance. The stimulation of VLDL-TG secretion is not driven by increased steatosis or decreased FA oxidation, but most likely by ChREBP mediated upregulation of *Fas* expression.

---

## Acknowledgements

This work was supported by grants from the Netherlands Organization for Scientific Research (NWO Zon-MW; 917.76.301 to P.J.V.) and the Dutch Diabetes Research Foundation (2005.01.003 to P.J.V.). M.C.W. is supported by a Mosaic grant of the Dutch Organization for Scientific Research (NWO 017.003.83). P.C.N.R. is an Established Investigator of the Netherlands Heart Foundation (2009T038). The authors are grateful to A. Logiantara for excellent technical assistance.

## References

- Cai D, Yuan M, Frantz DF, Melendez PA, Hansen L, Lee J, Shoelson SE. Local and systemic insulin resistance resulting from hepatic activation of IKK-beta and NF-kappaB. *Nat Med.* 2005;11:183-190.
- Arkan MC, Hevener AL, Greten FR, Maeda S, Li ZW, Long JM, Wynshaw-Boris A, Poli G, Olefsky J, Karin M. IKK-beta links inflammation to obesity-induced insulin resistance. *Nat Med.* 2005;11:191-198.
- Feingold KR, Soued M, Adi S, Staprans I, Shigenaga J, Doerrler W, Moser A, Grunfeld C. Tumor necrosis factor-increased hepatic very-low-density lipoprotein production and increased serum triglyceride levels in diabetic rats. *Diabetes.* 1990;39:1569-1574.
- Goldfine AB, Silver R, Aldhahi W, Cai D, Tatro E, Lee J, Shoelson SE. Use of salsalate to target inflammation in the treatment of insulin resistance and type 2 diabetes. *Clin Transl Sci.* 2008;1:36-43.
- Feingold KR, Staprans I, Memon RA, Moser AH, Shigenaga JK, Doerrler W, Dinarello CA, Grunfeld C. Endotoxin rapidly induces changes in lipid metabolism that produce hypertriglyceridemia: low doses stimulate hepatic triglyceride production while high doses inhibit clearance. *J Lipid Res.* 1992;33:1765-1776.
- van den Maagdenberg AM, Hofker MH, Krimpenfort PJ, de Bruijn I, van Vlijmen BJ, van der Boom H, Havekes LM, Frants RR. Transgenic mice carrying the apolipoprotein E3-Leiden gene exhibit hyperlipoproteinemia. *J Biol Chem.* 1993;268:10540-10545.
- Zadelaar S, Kleemann R, Verschuren L, de Vries-van der Weij J, van der Hoorn J, Princen HM, Kooistra T. Mouse models for atherosclerosis and pharmaceutical modifiers. *Arterioscler Thromb Vasc Biol.* 2007;27:1706-1721.
- Zambon A, Hashimoto SI, Brunzell JD. Analysis of techniques to obtain plasma for measurement of levels of free fatty acids. *J Lipid Res.* 1993;34:1021-1028.
- Bligh EG, Dyer WJ. A rapid method of total lipid extraction and purification. *Can J Biochem Physiol.* 1959;37:911-917.
- Folch J, Lees M, Sloane Stanley GH. A simple method for the isolation and purification of total lipides from animal tissues. *J Biol Chem.* 1957;226:497-509.
- Rensen PC, van Dijk MC, Havenaar EC, Bijsterbosch MK, Kruijt JK, van Berkel TJ. Selective liver targeting of antivirals by recombinant chylomicrons--a new therapeutic approach to hepatitis B. *Nat Med.* 1995;1:221-225.
- Rensen PC, Herijgers N, Netscher MH, Meskers SC, van Eck M, van Berkel TJ. Particle size determines the specificity of apolipoprotein E-containing triglyceride-rich emulsions for the LDL receptor versus hepatic remnant receptor in vivo. *J Lipid Res.* 1997;38:1070-1084.
- Jong MC, Rensen PC, Dahlmans VE, van der Boom H, van Berkel TJ, Havekes LM. Apolipoprotein C-III deficiency accelerates triglyceride hydrolysis by lipoprotein lipase in wild-type and apoE knockout mice. *J Lipid Res.* 2001;42:1578-1585.
- Redgrave TG, Roberts DC, West CE. Separation of plasma lipoproteins by density-gradient ultracentrifugation. *Anal Biochem.* 1975;65:42-49.
- Berry MN, Friend DS. High-yield preparation of isolated rat liver parenchymal cells: a biochemical and fine structural study. *J Cell Biol.* 1969;43:506-520.
- Groen AK, van Roermund CW, Vervoorn RC, Tager JM. Control of gluconeogenesis in rat liver cells. Flux control coefficients of the enzymes in the gluconeogenic pathway in the absence and presence of glucagon. *Biochem J.* 1986;237:379-389.
- Kuipers F, Jong MC, Lin Y, Eck M, Havinga R, Bloks V, Verkade HJ, Hofker MH, Moshage H, Berkel TJ, Vonk RJ, Havekes LM. Impaired secretion of very low density lipoprotein-triglycerides by apolipoprotein E-deficient mouse hepatocytes. *J Clin Invest.* 1997;100:2915-2922.
- Powell EE, Jonsson JR, Clouston AD. Steatosis: co-factor in other liver diseases. *Hepatology.* 2005;42:5-13.
- Khovidhunkit W, Kim MS, Memon RA, Shigenaga JK, Moser AH, Feingold KR, Grunfeld C. Effects of infection and inflammation on lipid and lipoprotein metabolism: mechanisms and consequences to the host. *J Lipid Res.* 2004;45:1169-1196.
- Hotamisligil GS. Inflammation and metabolic disorders. *Nature.* 2006;444:860-867.
- Rensen PC, Oosten M, Bilt E, Eck M, Kuiper J, Berkel TJ. Human recombinant apolipoprotein E redirects lipopolysaccharide from Kupffer cells to liver parenchymal cells in rats In vivo. *J Clin Invest.* 1997;99:2438-2445.
- Nonogaki K, Fuller GM, Fuentes NL, Moser AH, Staprans I, Grunfeld C, Feingold KR. Interleukin-6 stimulates hepatic triglyceride

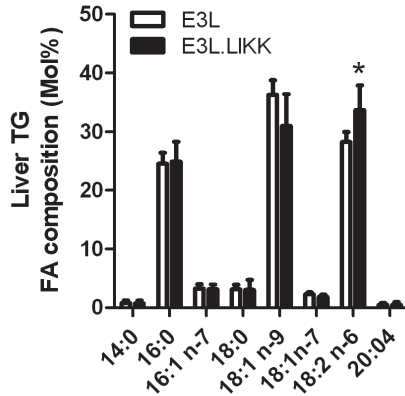
- secretion in rats. *Endocrinology*. 1995;136:2143-2149.
23. Tsai J, Zhang R, Qiu W, Su Q, Naples M, Adeli K. Inflammatory NF-kappaB activation promotes hepatic apolipoprotein B100 secretion: evidence for a link between hepatic inflammation and lipoprotein production. *Am J Physiol Gastrointest Liver Physiol*. 2009;296:G1287-G1298.
  24. Lewis GF, Steiner G. Acute effects of insulin in the control of VLDL production in humans. Implications for the insulin-resistant state. *Diabetes Care*. 1996;19:390-393.
  25. Huang W, Metlakunta A, Dedousis N, Zhang P, Sipula I, Dube JJ, Scott DK, O'Doherty RM. Depletion of liver Kupffer cells prevents the development of diet-induced hepatic steatosis and insulin resistance. *Diabetes*. 2010;59:347-357.
  26. Stienstra R, Saudale F, Duval C, Keshtkar S, Groener JE, van Rooijen N, Staels B, Kersten S, Muller M. Kupffer cells promote hepatic steatosis via interleukin-1beta-dependent suppression of peroxisome proliferator-activated receptor alpha activity. *Hepatology*. 2010;51:511-522.
  27. Glass CK, Ogawa S. Combinatorial roles of nuclear receptors in inflammation and immunity. *Nat Rev Immunol*. 2006;6:44-55.
  28. Stienstra R, Mandard S, Tan NS, Wahli W, Trautwein C, Richardson TA, Lichtenauer-Kaligis E, Kersten S, Muller M. The Interleukin-1 receptor antagonist is a direct target gene of PPARalpha in liver. *J Hepatol*. 2007;46:869-877.
  29. Watanabe M, Houten SM, Wang L, Moschetta A, Mangelsdorf DJ, Heyman RA, Moore DD, Auwerx J. Bile acids lower triglyceride levels via a pathway involving FXR, SHP, and SREBP-1c. *J Clin Invest*. 2004;113:1408-1418.
  30. Feingold KR, Soued M, Serio MK, Moser AH, Dinarello CA, Grunfeld C. Multiple cytokines stimulate hepatic lipid synthesis in vivo. *Endocrinology*. 1989;125:267-274.
  31. Grunfeld C, Verdier JA, Neese R, Moser AH, Feingold KR. Mechanisms by which tumor necrosis factor stimulates hepatic fatty acid synthesis in vivo. *J Lipid Res*. 1988;29:1327-1335.
  32. Joseph SB, Laffitte BA, Patel PH, Watson MA, Matsukuma KE, Walczak R, Collins JL, Osborne TF, Tontonoz P. Direct and indirect mechanisms for regulation of fatty acid synthase gene expression by liver X receptors. *J Biol Chem*. 2002;277:11019-11025.
  33. Iizuka K, Bruick RK, Liang G, Horton JD, Uyeda K. Deficiency of carbohydrate response element-binding protein (ChREBP) reduces lipogenesis as well as glycolysis. *Proc Natl Acad Sci U S A*. 2004;101:7281-7286.
  34. Kawaguchi T, Takenoshita M, Kabashima T, Uyeda K. Glucose and cAMP regulate the L-type pyruvate kinase gene by phosphorylation/dephosphorylation of the carbohydrate response element binding protein. *Proc Natl Acad Sci U S A*. 2001;98:13710-13715.
  35. Yamashita H, Takenoshita M, Sakurai M, Bruick RK, Henzel WJ, Shillinglaw W, Arnot D, Uyeda K. A glucose-responsive transcription factor that regulates carbohydrate metabolism in the liver. *Proc Natl Acad Sci U S A*. 2001;98:9116-9121.
  36. Morral N, Edenberg HJ, Witting SR, Altomonte J, Chu T, Brown M. Effects of glucose metabolism on the regulation of genes of fatty acid synthesis and triglyceride secretion in the liver. *J Lipid Res*. 2007;48:1499-1510.
  37. Grefhorst A, Elzinga BM, Voshol PJ, Plosch T, Kok T, Bloks VW, van der Sluijs FH, Havekes LM, Romijn JA, Verkade HJ, Kuipers F. Stimulation of lipogenesis by pharmacological activation of the liver X receptor leads to production of large, triglyceride-rich very low density lipoprotein particles. *J Biol Chem*. 2002;277:34182-34190.
  38. Chakravarthy MV, Pan Z, Zhu Y, Tordjman K, Schneider JG, Coleman T, Turk J, Semenkovich CF. "New" hepatic fat activates PPARalpha to maintain glucose, lipid, and cholesterol homeostasis. *Cell Metab*. 2005;1:309-322.

## Supplemental data

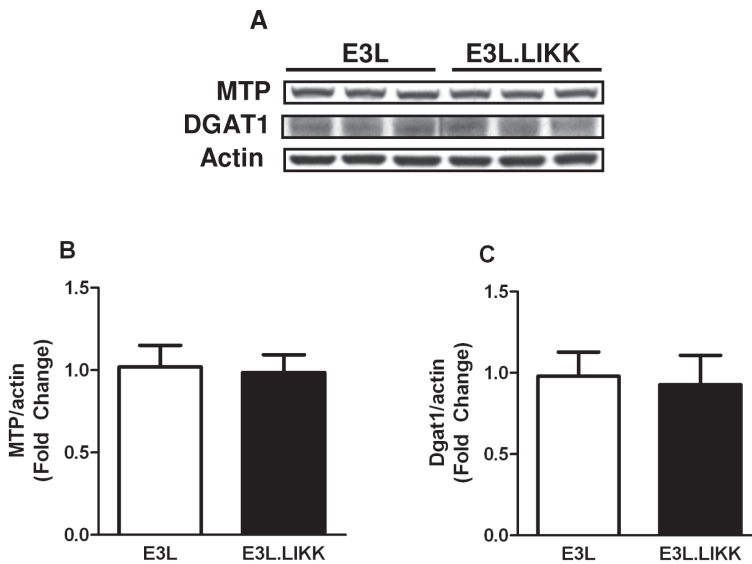
**Supplemental Table S1.** Primers used for quantitative real-time PCR analysis.

Gene	Forward primer	Reverse primer
<i>Abcg5</i>	TGTCCTACAGCGTCAGCAACC	GGCCACTCTCGATGTACAAGG
<i>Abcg8</i>	GACAGTTCACAGCCACAA	GCCTGAAGATGTCAGAGCGA
<i>Acox1</i>	TATGGGATCAGCCAGAAAGG	ACAGAGCCAAGGGTCACATC
<i>ApoB</i>	GCCCATTTGTGGACAAGTTGATC	CCAGGACTTGGAGGCTTTGGA
<i>Cidea</i>	CTCGGCTGTCTCAATGTCAA	CCGCATAGACCAGGAACCTGT
<i>Cidec</i>	CTGGAGGAAGATGGCACAAT	GGGCCACATCGATCTTCTTA
<i>Cpt1a</i>	GAGACTTCCAACGCATGACA	ATGGGTTGGGGTGTGTAGA
<i>Cyclo</i>	CAATGTCTGGACCAACACAA	GCCATCCAGCCATTCAGTCT
<i>Cyp27a1</i>	TCTGGCTACCTGCACTTCCT	CTGGATCTCTGGGCTCTTTG
<i>Cyp7a1</i>	CAGGGAGATGCTCTGTGTCA	AGGCATACATCCCTCCGTA
<i>Cyp8b1</i>	GGACAGCCTATCCTTGGTGA	CGGAACCTCCTGAACAGCTC
<i>Dgat1</i>	TCCGTCACAGGTGGTAGTG	TGAACAAAGAATCTGCAGACGA
<i>Fasn</i>	TCCTGGGAGGATGTAACAGC	CACAAATTCATTCACTGCAGCC
<i>Gapdh</i>	TGCAACCAACTGCTTAGC	GGCATGGACTGTGGTCATGAG
<i>Hmgcr</i>	CCGGCAACAACAAGATCTGTG	ATGTACAGGATGGCGATGCA
<i>Mttp</i>	CTCTTGGCAGTGCTTTTCTCT	GAGCTTGATAGCCGCTCATT
<i>Nr1h3</i>	CTGCACGCCTACGTCCAT	AAGTACGGAGGCTCACAGCT
<i>Nr1h4</i>	GGCCTCTGGTACCCTACA	ACATCCCCATCTCTTTGCAC
<i>Pklr</i>	GCAGAACGAGTCACAGCAAT	GTGGAGGCTTCTTCAAGTG
<i>Plin2</i>	CAGGATGGAGGAAAGACTGC	CTTATCCACCACCCTGAGA
<i>Plin5</i>	TGTCCAGTGTACAACCTCGG	CAGGGCACAGGTAGTCACAC
<i>Ppara</i>	ATGCCAGTACTGCCGTTTTTC	GGCCTTGACCTTGTTTCATGT
<i>Ppargc1b</i>	TTGTAGAGTGCCAGGTGCTG	CCTCCATAGCTCAGGTGGAA
<i>Srebp-1c</i>	GGAGCCATGGATTGCACATT	CCTGTCTCACCCCAGCATA

*Abcg5*, ATP-binding cassette sub-family G member 5; *Abcg8*, ATP-binding cassette sub-family G member 8; *Acox1*, acyl-coenzyme A oxidase 1; *ApoB*, apolipoprotein B; *Cidea*, cell death activator CIDE-A; *Cidec*, fat-specific protein FSP27; *Cpt1a*, carnitine palmitoyltransferase 1a; *Cyp27a1*, cholesterol 27 hydroxylase; *Cyp7a1*, cholesterol 7 alpha hydroxylase; *Cyp8b1*, sterol 12 alpha-hydroxylase; *Dgat1*, diglyceride acyltransferase 1; *Fas*, fatty acid synthase; *Hmgcr*, HMG-CoA reductase; *Mttp*, microsomal triglyceride transfer protein; *Nr1h3*, liver X receptor alpha; *Nr1h4*, farnesoid X activated receptor; *Pklr*, liver-type pyruvate kinase; *Plin2*, perilipin 2; *Plin5*, perilipin 5; *Ppara*, peroxisome proliferator activated receptor alpha; *Ppargc1b*, PPAR-gamma coactivator 1-beta; *Srebp-1c*, sterol-regulatory element binding protein.



**Supplemental Fig. S1.** Effect of *LIKK* on fatty acid composition of hepatic triglycerides in *E3L* mice. Livers were obtained from overnight fasted *E3L* and *E3L.LIKK* mice and lipids were extracted. TG were isolated by thin-layer chromatography followed by fatty acid separation and quantification using gas chromatography. Fatty acid composition was then determined (in mol%). Values are means  $\pm$  SD (n=5-7).



**Supplemental Fig. S2.** *LIKK* does not affect hepatic MTP and DGAT1 protein levels. *E3L* and *E3L.LIKK* mice were fed a chow diet and sacrificed at the age of 14 weeks after an overnight fast. MTP and DGAT1 levels were measured in liver tissue by Western blots and actin was used as an internal control. Representative Western blots are shown for 3 mice per group (A). Ratios of MTP (B) and DGAT1 (C) proteins over actin levels were quantified. Values are means  $\pm$  SD (n=5-7).

